Molecular-statistical description of the smectic-*A*–smectic-*C* phase transition

F. Gießelmann and P. Zugenmaier
Institute of Physical Chemistry, Technical University Clausthal, Arnold-Sommerfeld-Strasse 4, D-38678 Clausthal-Zellerfeld, Germany
(Received 16 January 1996; revised manuscript received 25 November 1996)

A simple molecular-statistical model of the smectic-*A*–smectic-*C* phase transition is proposed. Assuming a bilinear mean-field potential, the macroscopic tilt angle is calculated by Boltzmann statistics as a thermal average of the molecular tilt. The calculation leads to an equation of state for the smectic-*C* phase which is a self-consistent-field equation involving the Langevin function of a reduced tilt and a reduced temperature. This molecular-statistical approach of the smectic-*C*–smectic-*A* phase transition is in principle analogous to a ferromagnetic phase transition with spin number $S \to \infty$. An excellent description of experimental tilt angle data for the complete temperature range of the smectic-*C* phase is achieved with only one or two fit parameters, respectively. Differences between tilt angle data obtained by optical and by x-ray experiments originate from different moments of the tilt angle distribution function and from different interaction parameters for the mesogenic cores and the complete molecule. [S1063-651X(97)00504-7]

PACS number(s): 61.30.Cz, 64.70.Md

I. INTRODUCTION

Smectic-*A* (Sm-*A*) and smectic-*C* (Sm-*C*) liquid crystals are anisotropic fluids of, e.g., rod-shaped molecules exhibiting a long-range orientational order of the long molecular axis along the director $\hat{\vec{n}}$ and a quasilong-range positional order of the molecular centers of gravity in one dimension, which leads to a layered structure of period d along the smectic layer normal $\hat{\vec{z}}$ (cf. Fig. 1). A liquidlike positional order is found for all directions perpendicular to $\hat{\vec{z}}$. Sm-*A* and Sm-*C* phases exhibit the same fundamental structure involving two preferred directions in space, $\hat{\vec{n}}$ and $\hat{\vec{z}}$. The distinction between both phases is given by the mutual arrangement of $\hat{\vec{n}}$ and $\hat{\vec{z}}$: In the Sm-*A* phase the director $\hat{\vec{n}}$ and the smectic layer normal $\hat{\vec{z}}$ are parallel to each other, while in the Sm-*C* phase the director $\hat{\vec{n}}$ is inclined by a tilt angle Θ with respect to the layer normal $\hat{\vec{z}}$.

The thermodynamic state of liquid crystalline phases is described by the introduction of certain order parameters. The degree of axial orientational order is expressed by the Hermans orientational order parameter S [1],

$$S = \frac{1}{2}\langle 3\cos^2\alpha - 1\rangle, \tag{1}$$

with α being the angle between the individual long molecular axis and the director. The Hermans parameter S was adopted for liquid crystalline systems by Tsvetkov [2]. The degree of positional order in the z direction is described by a smectic order parameter σ,

$$\sigma = \left\langle \cos\left(\frac{2\pi}{d}z\right)\frac{3\cos^2\alpha - 1}{2}\right\rangle, \tag{2}$$

which was introduced by Kobayashi and McMillan [3–5]. The extent of director tilt is measured by the mean value of the molecular tilt represented by its magnitude $\vartheta \geqslant 0$ and its azimuthal tilt direction φ:

$$\left\langle \vartheta\begin{pmatrix}\cos\varphi\\ \sin\varphi\end{pmatrix}\right\rangle. \tag{3}$$

Assuming a uniform tilt direction, the absolute value $\Theta = \left|\langle \vartheta\binom{\cos\varphi}{\sin\varphi}\rangle\right|$, which is the macroscopic tilt angle Θ, may be considered as an order parameter. In the case of higher ordered smectics, further order parameters have to be defined.

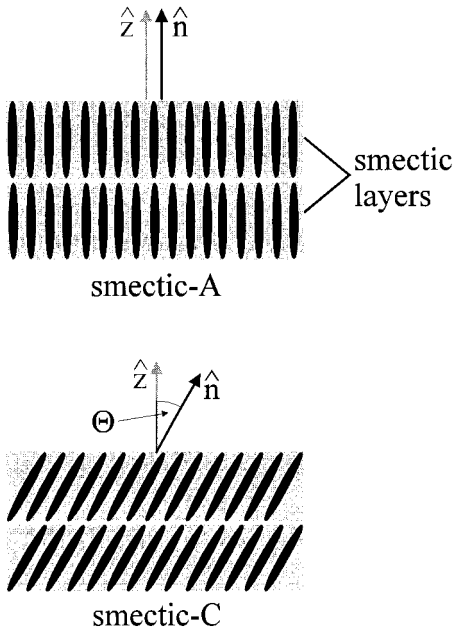

FIG. 1. Structural changes at the smectic-*A*–smectic-*C* phase transition: In the smectic-*C* phase the director $\hat{\vec{n}}$ is inclined by the tilt angle Θ with respect to the smectic layer normal $\hat{\vec{z}}$.

Liquid crystal phase transitions are characterized by a significant change of, at least, one order parameter which is the characteristic order parameter of that phase transition. Theories of phase transitions are expected to explain these order parameter changes. The characteristic order parameter for the first-order isotropic-nematic (N) phase transition is the orientational order parameter S. A statistical theory on this transition was first given by Born [6] in 1916. Born's theory, which was a molecular field approach similar to the Weiss theory of ferromagnetism, failed because it assumed a polar ordering of the molecular long axis thus neglecting the axial or pseudovector property of the director $\hat{\vec{n}}$. Today, the generally accepted molecular-statistical model of the nematic-isotropic transition is the Maier-Saupe theory [7], which explains the axial long-range orientational order by a mean-field approach based on induced dipole interactions. A phenomenological, Landau-type mean-field theory for the nematic-isotropic transition has been suggested by De Gennes [8]. The N–Sm-A transition, which may be of first or second order, is characterized by the smectic order parameter σ. Phenomenological and molecular-statistical approaches have been proposed by Kobayashi [3,4], McMillan [5], De Gennes [9,10], and Meyer and Lubensky [11].

The characteristic order parameter of the Sm-A–Sm-C transition is given by the macroscopic director tilt angle Θ. Early measurements by Taylor, Arora, and Fergason [12] on the temperature dependence of the tilt angle suggested that the Sm-A–Sm-C transition is a continuous, second-order phase transition. The molecular origin of the Sm-C tilt has not been conclusively clarified. Several models have been proposed explaining the Sm-C tilt by permanent dipole interactions (McMillan and De Jeu [13,14]), steric interactions (Wulf [15]) and permanent dipole-induced dipole interactions (Van der Meer and Vertogen [16]). Phenomenologically, the tilt angle is described by a Landau expansion of the free energy f about the phase transition temperature T_C,

$$f = f_0 + \frac{1}{2}\alpha(T - T_C)\Theta^2 + \frac{1}{4}b\Theta^4, \tag{4}$$

with temperature T, Landau coefficients α, b, and an additive constant f_0 representing the nonsingular part of f. This Landau-expansion was extended for chiral Sm-C^* phases by Žekš [17], considering the helicity and ferroelectricity of the Sm-C^* phase induced by chirality with the introduction of secondary order parameters.

Although the Landau expansion (4) gives a straightforward approach to many phenomena related to the Sm-A–Sm-C transition, its application involves various problems which are somehow unsatisfactory from a more rigid point of view. They are as follows.

(i) An *unusually large* sixth-order term $\frac{1}{6}c\Theta^6$ has to be added to the free energy expansion (4) in order to achieve a proper description of experimental results [18].

(ii) A slight temperature dependence of the coefficients b and c has to be assumed for a description of the Sm-C tilt far below the phase transition temperature T_C [19].

(iii) Due to the lack of a relevant molecular model, no physical interpretation of the Landau-expansion coefficients α, b, and c is available.

In this paper, we will present a rather simple statistical model which provides an excellent description of optical and x-ray tilt angle data for the complete Sm-C temperature range with a maximum of two fit parameters. The model might lead to an interpretation of the Landau coefficients, their temperature dependence, and the problems related to the unusually large sixth order term.

II. MOLECULAR-STATISTICAL MODEL

For further treatment it is useful to introduce a set of molecular tilt vectors $\vec{s}, \vec{s^2}, \ldots, \vec{s^n}$, which describe the tilt angle distribution of a Sm-C sample. The molecular tilt vectors are of lengths $\vartheta, \vartheta^2, \ldots, \vartheta^n$ (ϑ denotes the size of the molecular tilt) and point along the azimuthal direction $\hat{\vec{s}}$ of the molecular tilt:

$$\begin{aligned} \vec{s} &= \vartheta\hat{\vec{s}}, \\ \vec{s^2} &= \vartheta^2\hat{\vec{s}}, \\ &\vdots \\ \vec{s^n} &= \vartheta^n\hat{\vec{s}}; \quad \vartheta \geqslant 0 \end{aligned} \tag{5}$$

with

$$\hat{\vec{s}} = \begin{pmatrix} \cos\varphi \\ \sin\varphi \end{pmatrix}, \quad -\pi \leqslant \varphi \leqslant \pi. \tag{6}$$

The azimuthal angle φ of the molecular tilt is measured towards the positive direction of the x axis, which is orthogonal to the layer normal $\hat{\vec{z}}$. Defining the mean tilt direction as the positive direction of the x axis ($\varphi = 0$), the various moments of the tilt angle distribution function result from

$$\begin{aligned} \langle\Theta\rangle &= |\langle\vec{s}\rangle| = \langle\vartheta\hat{\vec{s}}\rangle, \\ \langle\Theta^2\rangle &= |\langle\vec{s^2}\rangle| = \langle\vartheta^2\hat{\vec{s}}\rangle, \\ &\vdots \\ \langle\Theta^n\rangle &= |\langle\vec{s^n}\rangle| = \langle\vartheta^n\hat{\vec{s}}\rangle. \end{aligned} \tag{7}$$

The macroscopic tilt angle $\langle\Theta\rangle$, the mean square tilt angle $\langle\Theta^2\rangle$, and higher moments are obtained as the absolute magnitude of the average molecular tilt vectors.

A. Assumptions

Within the notation given in Eqs. (5)–(7), our statistical model is based on the following assumptions.

(i) The individual molecular tilt angle ϑ is restricted to a finite range (Fig. 2) limited by a maximum molecular tilt angle Ω:

$$0 \leqslant \vartheta \leqslant \Omega. \tag{8}$$

The borderline angle Ω is considered to be a fixed quantity which essentially remains constant. A physical interpretation

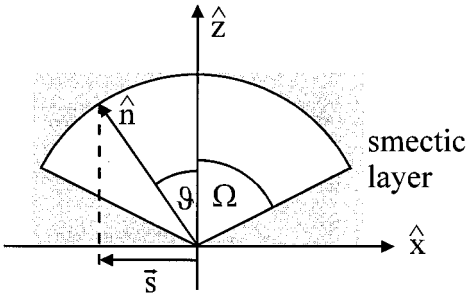

FIG. 2. Basic assumptions of the molecular-statistical model: The individual molecular tilt angle ϑ is limited to a finite range $0 \leqslant \vartheta \leqslant \Omega$. The size and the direction of the molecular tilt is expressed by the tilt vector $\vec{s}$, which is the projection of the molecular director $\hat{\vec{n}}$ onto the smectic layer plane with length $\sin\vartheta \approx \vartheta$. The unit vector $\hat{\vec{z}}$ denotes the smectic layer normal.

of Ω might be given by the tilt angle of the Sm-*C* phase in the absence of any thermal energy, e.g., if the phase is supercooled to zero temperature.

(ii) The potential U of a single molecule with tilt vector $\vec{s}$ in the environment of its surrounding molecules with mean tilt vector $\langle\vec{s}\rangle$ is given by the bilinear ansatz

$$U(\vec{s}) = -\lambda\langle\vec{s}\rangle\cdot\vec{s} \tag{9}$$

with the mean-field coefficient $\lambda > 0$. The physical content of this ansatz is illustrated in Fig. 3: If the single molecule fits to its neighboring molecules, which means that the individual tilt vector $\vec{s}$ and the mean-tilt vector $\langle\vec{s}\rangle$ are parallel, the potential is low ($U<0$). If the single molecule disturbs the local ordering, especially if $\vec{s}$ and $\langle\vec{s}\rangle$ are antiparallel, the potential is high ($U>0$). The tilt vector $\vec{s}$ formally acts as a *sterical dipole* [20] which couples to an internal *tilting field* represented by the mean tilt vector $\langle\vec{s}\rangle$. In a first approximation, the mean-field coefficient λ should be considered as a quantity, essentially independent of temperature.

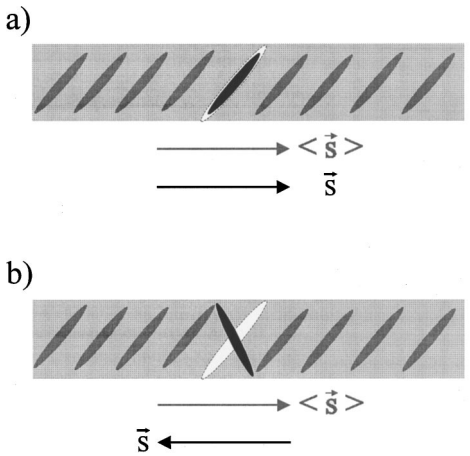

FIG. 3. Physical content of the mean-field ansatz given by Eq. (9): $\vec{s}$ is the tilt vector of an individual molecule and $\langle\vec{s}\rangle$ gives the mean tilt direction of its neighboring molecules. If both vectors are parallel, the individual molecule fits to the sorrounding molecules and the potential is low (a). The potential is high if $\vec{s}$ and $\langle\vec{s}\rangle$ are antiparallel (b).

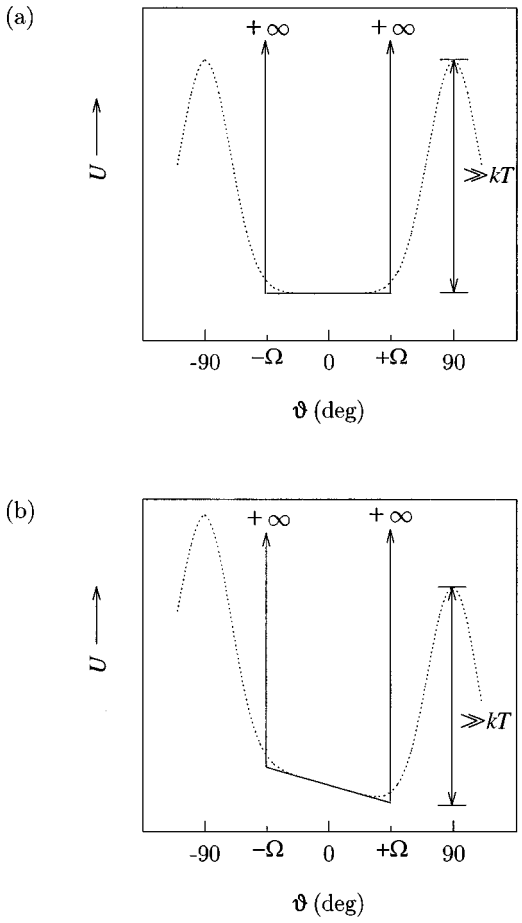

FIG. 4. Discussion of the mean-field potential U for the tilt of an individual molecule within a smectic layer by an angle ϑ in the Sm-*A* (a) and the Sm-*C* (b) phase. The mean field potential (solid lines) is a rough approximation of a more realistic potential (dotted lines) by a simple box potential, considering the borderline case of hard-rod repulsion with infinite potential walls at the borderline angle $\pm\Omega$. For explanations, see the text.

An improved understanding of the borderline angle Ω can be obtained by a discussion of the mean-field potential (Fig. 4): Rotating a single molecule within a smectic layer environment by an angle ϑ, a strong steric repulsion takes place if ϑ approaches a certain angle ($\pm\Omega$), which means that the $+\hat{\vec{n}}$ and $-\hat{\vec{n}}$ directions of an individual molecule within a smectic layer are separated by high potential barriers with $\Delta U \gg kT$. Between these walls, the potential is more or less flat, which leads to the well known thermal tilt fluctuations of smectic-*A* and smectic-*C* molecules. This potential is schematically depicted by the dotted lines in Fig. 4. The mean-field potential used in our model includes nothing but a rough approximation of the real potential by a simple box potential, considering the borderline case of hard-rod repulsion with infinite potential walls at $\pm\Omega$.

(iii) The consideration may be simplified by the restriction of the 2π tilt degeneracy to only two antiparallel tilt directions, e.g., $\varphi = 0$ and $\varphi = \pi$. With this assumption the two-component tilt vector $\vec{s}$ [cf. Eqs. (5) and (6)] reduces to a one-dimensional tilt vector with directions

$$\hat{\vec{s}} = s - \{-1, +1\}. \tag{10}$$

This assumption is justified by the fact that the tilt direction Φ is a gauge variable, which has no thermodynamically predetermined value at all [21]. Only gradients $\nabla\Phi$ contribute to the free energy on an energy scale far below kT. Therefore, Φ may be considered as a hydrodynamic variable, not as a thermodynamic (hard) variable. Consequently, the Φ fluctuations are not relevant for the thermodynamics of the phase transition. If Θ and Φ fluctuations are well separated on the energy scale, it is possible to separate the averaging over both variables. In this case, the discretization of $\hat{\vec{s}}$ may be considered as the result of the Φ averaging with $\vec{s} = +1$ representing the mean tilt direction. The opposite tilt direction has to be included for reasons of symmetry. Otherwise, no smectic-*A* state with equally distributed tilt directions and $\langle\Theta\rangle = 0$ can be described.

(iv) The expectation values of the macroscopic tilt $\langle\Theta\rangle$ and the higher moments $\langle\Theta^2\rangle, \ldots, \langle\Theta^n\rangle$ of the tilt angle distribution function are calculated from the microscopic tilt vectors by application of the Boltzmann statistics.

With these assumptions the macroscopic tilt angle and the higher moments of its distribution function are calculated in the next section.

B. Mean values and equation of state

1. General expression for the nth moment

Applying Eqs. (5), (8), and (10) to Eq. (9), the mean-field potential reads

$$U(\vartheta, \hat{\vec{s}}) = -\lambda \langle \vartheta \hat{\vec{s}} \rangle \cdot \vartheta \hat{\vec{s}}. \tag{11}$$

Remembering that the average molecular tilt $\langle \vartheta \hat{\vec{s}} \rangle$ defines the macroscopic tilt $\langle\Theta\rangle$ in the positive x direction, Eq. (11) may also be written as

$$U(\vartheta, s) = -\lambda \langle\Theta\rangle \vartheta s. \tag{12}$$

The single-particle distribution function reads using Boltzmann statistics

$$f_B(\vartheta, s) = C^{-1} \exp\left(\frac{\lambda \langle\Theta\rangle \vartheta s}{kT} \right) \tag{13}$$

with normalization constant C:

$$C = \int_s \int_\vartheta f_B(\vartheta, s)\, d\vartheta\, ds. \tag{14}$$

The nth moment of the tilt angle distribution function $\langle\Theta^n\rangle = \langle \vartheta^n s \rangle$ [Eq. (7)] results in

$$\langle\Theta^n\rangle = \frac{\int_s \int_\vartheta [\vartheta^n s f_B(\vartheta, s)]\, d\vartheta\, ds}{\int_s \int_\vartheta f_B(\vartheta, s)\, d\vartheta\, ds}. \tag{15}$$

The application of the third assumption allows us to replace the outer integral over the tilt directions $\hat{\vec{s}}$ by a sum over the discrete tilt directions:

$$\langle\Theta^n\rangle = \frac{\sum_s \left\{ s \cdot \int_\vartheta [\vartheta^n f_B(\vartheta, s)]\, d\vartheta \right\}}{\sum_s \left\{ \int_\vartheta f_B(\vartheta s)\, d\vartheta \right\}}. \tag{16}$$

Inserting $s = \{+1, -1\}$ [Eq. (10)] and the distribution function [Eq. (13)] and specifying the integration range for ϑ according to the first assumption [Eq. (8)], we obtain the general expression

$$\langle\Theta^n\rangle = \frac{\int_0^\Omega \vartheta^n \exp\left(\frac{\lambda \langle\Theta\rangle \vartheta}{kT} \right) d\vartheta - \int_0^\Omega \vartheta^n \exp\left(-\frac{\lambda \langle\Theta\rangle \vartheta}{kT} \right) d\vartheta}{\int_{-\Omega}^\Omega \exp\left(\frac{\lambda \langle\Theta\rangle \vartheta}{kT} \right) d\vartheta}. \tag{17}$$

The first integral in the numerator of this expression is related to molecular orientations tilted in the positive x direction ($s = +1$), the second one to molecular orientations tilted in the negative x direction ($s = -1$). The corresponding integrals in the denominator are combined by a shift of the integration limits.

2. First moment: Macroscopic tilt angle

The first moment or the linear average of the tilt angle distribution function is the macroscopic tilt angle $\langle\Theta\rangle$ and calculated from Eq. (17) with $n = 1$:

$$\langle\Theta\rangle = \frac{\int_0^\Omega \vartheta \exp\left(\frac{\lambda \langle\Theta\rangle \vartheta}{kT} \right) d\vartheta - \int_0^\Omega \vartheta \exp\left(-\frac{\lambda \langle\Theta\rangle \vartheta}{kT} \right) d\vartheta}{\int_{-\Omega}^\Omega \exp\left(\frac{\lambda \langle\Theta\rangle \vartheta}{kT} \right) d\vartheta} = \frac{\int_{-\Omega}^\Omega \vartheta \exp\left(\frac{\lambda \langle\Theta\rangle \vartheta}{kT} \right) d\vartheta}{\int_{-\Omega}^\Omega \exp\left(\frac{\lambda \langle\Theta\rangle \vartheta}{kT} \right) d\vartheta} = \Omega \mathcal{L}(a\Omega). \tag{18}$$

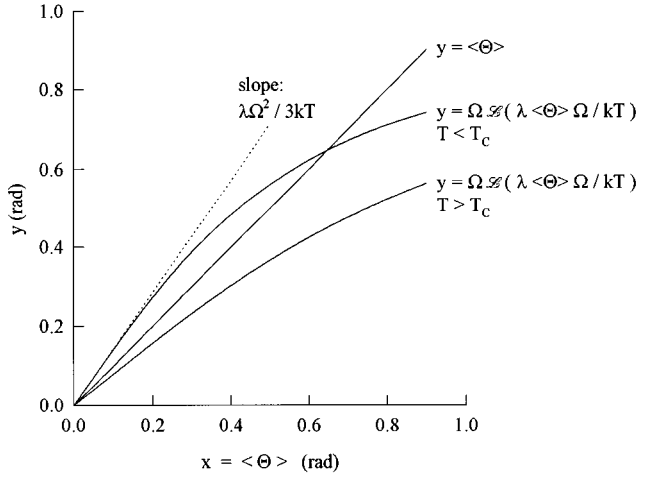

FIG. 5. Graphical solution of the self-consistent-field equation (19). For explanations, see the text.

Substituting $a=\lambda\langle\Theta\rangle/kT$ and carrying out the integration, the right-hand side of Eq. (18) simply reduces to the Langevin function $\mathcal{L}(a\Omega)$. After resubstitution Eq. (18) reads

$$\langle\Theta\rangle=\Omega\left(\coth\left(\frac{\lambda\langle\Theta\rangle\Omega}{kT}\right)-\frac{1}{\left(\frac{\lambda\langle\Theta\rangle\Omega}{kT}\right)}\right)=\Omega\mathcal{L}\left(\frac{\lambda\langle\Theta\rangle\Omega}{kT}\right). \tag{19}$$

Equation (19) is a self-consistent-field equation (SCF) for $\langle\Theta\rangle$. The macroscopic tilt angle $\langle\Theta\rangle$ is expressed as a function of temperature T by the real solutions of Eq. (19).

3. Equation of state

Following the treatment of Weiss [22], the SCF equation (19) can be solved graphically by plotting the left-hand and the right-hand sides of Eq. (19) as a function of $\langle\Theta\rangle$ (Fig. 5). The trivial solution $\langle\Theta\rangle=0$ represents the Sm-*A* phase. A further, nontrivial solution exists, if the initial slope of the right-hand-side function $\frac{1}{3}(\lambda\Omega^2/kT)$, which results from the Taylor expansion of the Langevin function, exceeds the initial slope of the left-hand-side function, which is simply 1. The borderline case represents the Sm-*A*–Sm-*C* phase transition into the tilted phase with the transition temperature T_C,

$$1=\frac{1}{3}\frac{\lambda\Omega^2}{kT_C},$$

and the mean-field coefficient λ is obtained by

$$\lambda=\frac{3k}{\Omega^2}T_C. \tag{20}$$

Substitution of the mean-field coefficient in the SCF equation (19) leads to

$$\langle\Theta\rangle=\Omega\mathcal{L}\left(3\frac{T_C}{T}\frac{\langle\Theta\rangle}{\Omega}\right). \tag{21}$$

Introducing the reduced temperature τ,

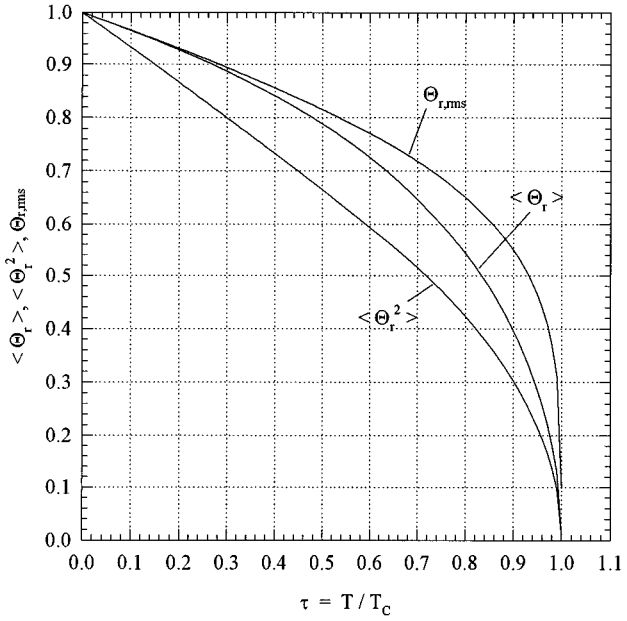

FIG. 6. General results for the reduced values of the macroscopic tilt $\langle\Theta_r\rangle$ [first moment, Eq. (24)], the reduced mean square tilt $\langle\Theta_r^2\rangle$ [second moment, Eq. (28)], and the root per mean square tilt $\langle\Theta_{r,\mathrm{rms}}\rangle$ as a function of the reduced temperature $\tau=T/T_C$ with temperature T and phase transition temperature T_C.

$$\tau=\frac{T}{T_C}, \tag{22}$$

and the reduced tilt $\langle\Theta_r\rangle$,

$$\langle\Theta_r\rangle=\frac{\langle\Theta\rangle}{\Omega}, \tag{23}$$

a very simple *equation of state* is obtained for the Sm-*C* phase:

$$\langle\Theta_r\rangle=\mathcal{L}\left(3\frac{\langle\Theta_r\rangle}{\tau}\right). \tag{24}$$

The equation of state (24) can be solved numerically. The general result is depicted in Fig. 6. It clearly describes a second order phase transition with $\langle\Theta_r\rangle=0$ for $T\geqslant T_C$ ($\tau\geqslant 1$) and a steep but continuous increase of $\langle\Theta_r\rangle$ for $T<T_C$ ($\tau<1$).

The numerical solutions of the equation of state (24) may be approximated by an expansion of the Langevin function up to the fifth order of $\langle\Theta_r\rangle$,

$$\langle\Theta_r\rangle\approx\frac{1}{\tau}\langle\Theta_r\rangle-\frac{3}{5\tau^3}\langle\Theta_r\rangle^3+\frac{18}{35\tau^5}\langle\Theta_r\rangle^5$$

$$0\approx\left(\frac{1}{\tau}-1\right)-\frac{3}{5\tau^3}\langle\Theta_r\rangle^2+\frac{18}{35\tau^5}\langle\Theta_r\rangle^4 \tag{25}$$

with the real, positive solution of Eq. (25) given by:

$$\langle\Theta_r\rangle\approx\frac{1}{6}(21\tau^2-3\sqrt{280\tau^5-231\tau^4})^{1/2}. \tag{26}$$

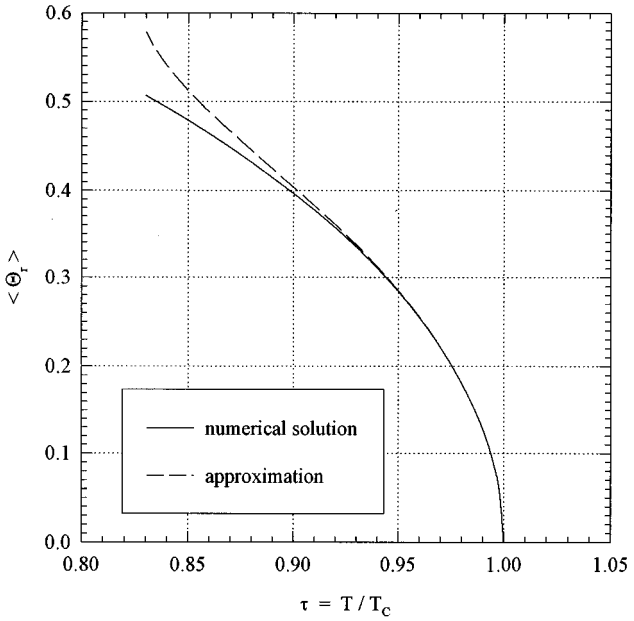

FIG. 7. Approximation of the numerial solution of the equation of state (24) by Eq. (26) in the vicinity of the phase transition. The reduced macroscopic tilt $\langle\Theta_r\rangle$ is plotted vs the reduced temperature τ.

This approximation is compared to the numerical solution of the equation of state (24) in Fig. 7 leading to the conclusion that this approximation is valid for a reduced temperature range of $0.9 \leqslant \tau \leqslant 1$. Assuming a phase transition temperature of $T_C \approx 350$ K, the reduced temperature $\tau = 0.9$ corresponds to $T_C - T = 35$ K, which is a sufficient range of validity for the description of most Sm-*C* phases.

4. Second moment: Mean square tilt angle

The second moment of the tilt angle distribution function or the mean square tilt angle is calculated by Eq. (17) with $n=2$:

$$\langle\Theta^2\rangle = \frac{\int_0^\Omega \vartheta^2 \exp\left(\frac{\lambda\langle\Theta\rangle\vartheta}{kT}\right) d\vartheta - \int_0^\Omega \vartheta^2 \exp\left(-\frac{\lambda\langle\Theta\rangle\vartheta}{kT}\right) d\vartheta}{\int_{-\Omega}^{\Omega} \exp\left(\frac{\lambda\langle\Theta\rangle\vartheta}{kT}\right) d\vartheta}$$

$$= \Omega^2 \left\{ \begin{array}{l} \left[1 + \dfrac{2}{\left(\dfrac{\lambda\langle\Theta\rangle\Omega}{kT}\right)^2}\right] \coth\left(\dfrac{\lambda\langle\Theta\rangle\Omega}{kT}\right) \\ - \dfrac{2}{\dfrac{\lambda\langle\Theta\rangle\Omega}{kT}} - \dfrac{2}{\left(\dfrac{\lambda\langle\Theta\rangle\Omega}{kT}\right)^2 \sinh\left(\dfrac{\lambda\langle\Theta\rangle\Omega}{kT}\right)} \end{array} \right\}. \tag{27}$$

Substituting λ by Eq. (20) and introducing the reduced variables $\langle\Theta_r\rangle$ and τ [Eqs. (22) and (23)] we obtain

$$\langle\Theta_r^2\rangle = \left(1 + \frac{2\tau^2}{9\langle\Theta_r\rangle^2}\right) \coth\left(\frac{3\langle\Theta_r\rangle}{\tau}\right) - \frac{2\tau}{3\langle\Theta_r\rangle} - \frac{2\tau^2}{9\langle\Theta_r\rangle^2 \sinh\left(\frac{3\langle\Theta_r\rangle}{\tau}\right)}. \tag{28}$$

The reduced mean square tilt $\langle\Theta_r^2\rangle$ was calculated from the $\langle\Theta_r\rangle$ values obtained from the numerical solution of the equation of state. The results are plotted in Fig. 6.

The reduced values of the root per mean square tilt $\Theta_{r,\mathrm{rms}}$ are calculated by

$$\Theta_{r,\mathrm{rms}} = \sqrt{\langle\Theta_r^2\rangle} \tag{29}$$

and also plotted in Fig. 6. As shown in Fig. 6, the three averages $\langle\Theta_r\rangle$, $\langle\Theta_r^2\rangle$, and $\Theta_{r,\mathrm{rms}}$ are related for all reduced teperatures τ by the inequality

$$\langle\Theta_r^2\rangle \leqslant \langle\Theta_r\rangle \leqslant \Theta_{r,\mathrm{rms}}. \tag{30}$$

An approximation for the mean square tilt is obtained by expanding the right-hand side of Eq. (28):

$$\langle\Theta_r^2\rangle = \frac{3}{4\tau}\langle\Theta_r\rangle - \frac{3}{8\tau^3}\langle\Theta_r\rangle^3 + \cdots. \tag{31}$$

For small values of $\langle\Theta_r\rangle$, the mean square tilt $\langle\Theta_r^2\rangle$ depends linearly on $\langle\Theta_r\rangle$,

$$\langle\Theta_r^2\rangle \approx \frac{3}{4\tau}\langle\Theta_r\rangle \tag{32}$$

and the root per mean square tilt increases with the square root of $\langle\Theta_r\rangle$:

$$\Theta_{r,\mathrm{rms}} \approx \frac{\sqrt{3}}{2}\sqrt{\frac{\langle\Theta_r\rangle}{\tau}}. \tag{33}$$

As we will show later, the various tilt averages are obtained by tilt angle measurements with different experimental techniques.

III. EXPERIMENTAL DATA

In this section the molecular-statistical model will be applied to experimental data. First, we will discuss the number and the nature of fit parameters involved by this model. Subsequently, the question will be addressed as to which experimental technique will be used to measure what moment of the tilt angle distribution. Finally, the model will be applied to fit tilt angle data of various sources, obtained by various experimental techniques.

A. Fit parameters and refinement

The equation of state (24) and the related equations (28) and (29) are formulated in terms of the reduced variables of state Θ_r and τ. Strictly speaking, they describe a situation of *corresponding states*, resulting in a unified description which should be valid for all Sm-*C* phases. Consequently, these equations involve *no* fit parameter.

These reduced quantities are not available by an experiment. With the definition of the reduced tilt angle given by Eq. (23), the various tilt averages are obtained from the reduced quantities by

$$\langle\Theta\rangle=\Omega\langle\Theta_r\rangle, \tag{34}$$

$$\langle\Theta^2\rangle=\Omega^2\langle\Theta_r^2\rangle, \tag{35}$$

$$\Theta_{\mathrm{rms}}=\Omega\Theta_{r,\mathrm{rms}}. \tag{36}$$

For any temperature ratio T/T_C the values of $\langle\Theta_r\rangle$,$\langle\Theta_r^2\rangle$, and $\Theta_{r,\mathrm{rms}}$ are given by the solution of the equation of state (Fig. 6). The one and only fit parameter involved by the model is the maximum tilt angle of the indvidual molecule Ω.

In systems with low dimensionality ($d<4$), mean-field theory provides only a first approximation of critical phenomena. In order to improve the fitting of the theory to experiments, the mean-field approach is usually refined by the introduction of a temperature-dependent potential strength $\lambda(T)$ (e.g., by Gerlach [23] for the Weiss theory and by Chandrasekhar and Madhusudana [24] and Humphries, James, and Luckhurst [25] for the Maier-Saupe theory). This refinement gives some corrections to basic lacks of mean-field theory which neglects the effects of the following: (i) thermal expansion, changing the packing density and the intermolecular distance r; (ii) fluctuations of the mean field due to short range interactions, which are important close to the phase transition; and (iii) higher order terms in the mean-field potential [e.g., a third order term in Eq. (9)], which might become evident at high values of the order parameter far below the phase transition.

These effects are reflected by an apparent temperature dependence of the mean-field coefficient $\lambda(T)$. Assuming a constant temperature coefficient α_V, $\lambda(T)$ may be written as

$$\lambda=\frac{\lambda_0}{1+\alpha_V(T-T_C)} \tag{37}$$

with λ_0 being the mean-field coefficient at the phase transition ($T=T_C$). With this ansatz, the refined equation of state reads

$$\langle\Theta_r\rangle=\mathscr{L}\left(3\frac{\langle\Theta_r\rangle}{\tau[1+\alpha_V(T-T_C)]}\right). \tag{38}$$

Introducing an apparent reduced temperature τ_{app},

$$\tau_{\mathrm{app}}=\tau[1+\alpha_V(T-T_C)], \tag{39}$$

the refined approach, Eq. (38), is written as

$$\langle\Theta_r\rangle=\mathscr{L}\left(3\frac{\langle\Theta_r\rangle}{\tau_{\mathrm{app}}}\right). \tag{40}$$

Equation (40) suggests that the effect of a temperature-dependent mean-field coefficient is transformed on a different temperature scale given by τ_{app}: An increase of the interaction coefficient has the same effect on the ordering as a decrease of the reduced temperature reflected by $\tau_{\mathrm{app}}<\tau$ for $\alpha_V>0$. This refined approach involves two fit parameters: Ω and α_V. A more detailed interpretation of $\lambda(T)$ and its temperature coefficient α_V cannot be discussed within the framework of classical mean-field theory and needs more sophisticated models including short range interactions and fluctuation effects.

In these considerations, the phase transition temperature T_C was *not* treated as a fit parameter because its value may be easily determined by experimental observation. Of course, the fitting procedure may be executed to allow an adjustment of the experimentally determined value within the typical range of experimental errors of about ± 1 K.

B. Experimental relevance of the various tilt averages

If the director tilt angle is considered as a dynamic quantity which undergoes statistical fluctuations in general, it has to be checked which experimental technique leads to a certain average (moment) of the tilt angle distribution function. The Sm-C tilt angle is experimentally determined by optical or x-ray methods. Optical measurements are carried out by conoscopical observation parallel to the smectic layer normal or by measuring the orientation of a homogeneously aligned sample (director perpendicular to the light propagation) which led to an extinction between crossed polars. These optical methods basically probe the direction of the optical axis, which is given by the main axis of the dielectric tensor at optical frequencies. Therefore, the optical tilt angle Θ_{opt} is related to the linear average $\langle\Theta\rangle$ of the tilt angle distribution function:

$$\Theta_{\mathrm{opt}}=\langle\Theta\rangle=\Omega\langle\Theta_r\rangle. \tag{41}$$

The x-ray measurement of the Sm-C tilt is carried out by comparing the smectic layer spacing d_C of the Sm-C phase with the layer spacing of the Sm-A phase d_A, which leads to the cosine of the tilt angle Θ:

$$\cos\Theta=\frac{d_C}{d_A}. \tag{42}$$

Orientational fluctuations of the long molecular axis, given by the main axis of the molecular principal axis of inertia, lead to fluctuations of the smectic layer thickness which are linearly averaged during the x-ray experiment, and Eq. (42) should be rewritten as

$$\langle\cos\Theta\rangle=\frac{\langle d_C\rangle}{\langle d_A\rangle}. \tag{43}$$

Therefore, the x-ray experiment measures the cosine average of the tilt angle, which is related to the even moments $\langle\Theta^2\rangle$, $\langle\Theta^4\rangle$, . . . of the tilt angle distribution function:

$$\langle\cos\Theta\rangle=\left\langle 1-\frac{\Theta^2}{2}+\cdots\right\rangle=1-\frac{\langle\Theta^2\rangle}{2}+\cdots. \tag{44}$$

The x-ray tilt angle $\Theta_{\mathrm{x\ ray}}$ is calculated by

$$\begin{aligned}\Theta_{\mathrm{x\ ray}}&=\arccos(\langle\cos\Theta\rangle)\\&=\arccos\left(1-\frac{\langle\Theta^2\rangle}{2}+\cdots\right)=\sqrt{\langle\Theta^2\rangle}-\frac{1}{24}(\sqrt{\langle\Theta^2\rangle})^3+\cdots\\&\approx\sqrt{\langle\Theta^2\rangle}.\end{aligned} \tag{45}$$

Consequently, the x-ray tilt angle $\Theta_{\text{x ray}}$ is related in a first approximation to the root per mean square tilt angle Θ_{rms}:

$$\Theta_{\text{x ray}} \approx \Theta_{\text{rms}} = \Omega \Theta_{r,\text{rms}}. \tag{46}$$

In fact, experiments often show a pronounced difference between optical and x-ray tilt angles with respect to the size and the temperature dependence of the tilt. These differences are explained in the framework of our model by the following considerations.

(i) *Influence of the maximum tilt* Ω. Generally, the principal axis of the molecular polarizability tensor and the molecular tensor of inertia do not coincide. Following this argument, the maximum tilt angle of the molecular optical axis (principal axis of the polarizability tensor) Ω_{opt} differs from the maximum tilt angle of the molecular long axis (principal axis of inertia) $\Omega_{\text{x ray}}$ and Eqs. (41) and (46) can be rewritten as

$$\Theta_{\text{opt}} = \Omega_{\text{opt}} \langle \Theta_r \rangle, \tag{47}$$

$$\Theta_{\text{x ray}} = \Omega_{\text{x ray}} \Theta_{r,\text{rms}}. \tag{48}$$

(ii) *Influence of the tilt distribution*. Substituting $\langle \Theta_r \rangle$ and $\Theta_{r,\text{rms}}$ in Eq. (33) by Eqs. (47) and (48) we obtain

$$\Theta_{\text{x ray}} = \sqrt{\frac{3\Omega_{\text{x ray}}^2}{4\tau\Omega_{\text{opt}}}\Theta_{\text{opt}}}. \tag{49}$$

Roughly speaking, the x-ray tilt is proportional to the square root of the optical tilt at the same reduced temperature τ and τ_{app}, respectively. The proportionality depends on the magnitude of $\Omega_{\text{x ray}}$ and Ω_{opt}.

(iii) *Influence of the interaction coefficient* $\lambda(T)$. Packing density and short range interactions might be quite different for the mesogenic core and the flexible tails of the liquid crystal molecule. Therefore, the interaction coefficient $\lambda(T)$ observed depends on the part of the molecule considered: The tilt of the mesogens related to the optical tilt or the tilt of the complete molecule probed by the x-ray tilt angle.

The analysis of experimental data given in the following section leads to the conclusion that the last two points seem to be most important for the interpretation of the differences between optical and x-ray tilt angles.

C. Measurements and fits

Our model outlined in the preceding sections is tested with some measurements of Sm-*C* tilt angles which are well established in literature. The first series of measurements were taken on terephthal-bis(4*n*)-butylaniline (TBBA). Taylor, Arora, and Fergason measured the optical tilt angle of TBBA by conoscopy [12] and x-ray measurements on the tilt angle of TBBA were reported by Kumar [26]. The data were taken from literature and plotted in Fig. 8. The phase transition temperature T_C reported by Kumar [26] was about 3 K lower than the value measured by Fergason *et al.* [12]. In order to give a consistent analysis of both tilt angle data sets, we decided to add 3 K to the temperatures given by Kumar. The optical and the x-ray tilt angle of 4-hexyloxy-salicylidene-4′-heptylaniline (HSHA) were measured by Ostrovskii [27]. These data are also reported in a monography by Blinov and Chigrinov [28] and plotted in Fig. 9.

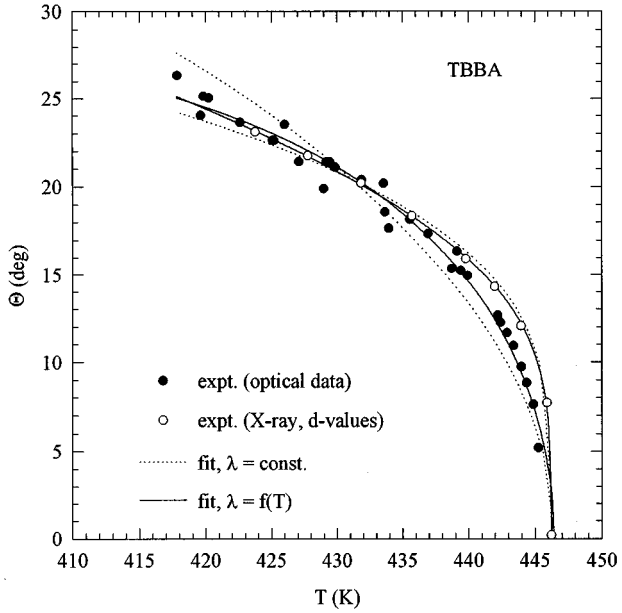

FIG. 8. Optical and x-ray tilt angle data of terephtal-bis (4*n*)-butylaniline (TBBA). The data are fitted by the molecular-statistical model as linear (optical) and root per mean square (x-ray) averages of the tilt angle distribution function. Dotted lines refer to one-parameter fits with mean-field coefficient λ independent from temperature *T*. The solid lines represent two-parameter fits assuming a temperature variation of λ. The data are taken from Refs. [12] and [26]. Fit parameters are listed in Table I.

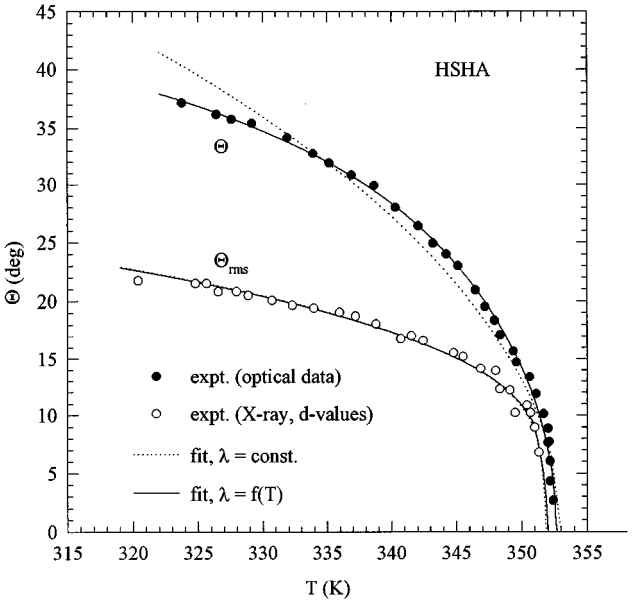

FIG. 9. Optical and x-ray tilt angle data of 4-hexyloxy-salicylidene-4′-heptylaniline (HSHA). The data are fitted by the molecular-statistical model as linear (optical) and root per mean square (x-ray) averages of the tilt angle distribution function. Dotted lines refer to one-parameter fits with mean-field coefficient λ independent of temperature *T*. The solid lines represent two-parameter fits assuming a temperature variation of λ. The data are taken from Ref. [28]. Fit parameters are listed in Table I.

TABLE I. Fit parameters and related quantities obtained for the molecular-statistical model of the Sm-A–Sm-C phase transition of TBBA and HSHA.

Compound	Method	Ref.	T_C (K)	Ω (deg)	α_V (10^{-3} K^{-1})	λ_0 (10^{-20} J)
TBBA	optical	[12]	446.3	25.3	35.2	9.5
TBBA	x ray	[26]	446.2	32.3	7.14	5.8
HSHA	optical	[28]	352.6	40.0	27.9	3.0
HSHA	x ray	[28]	351.9	44.7	−0.9	2.4

The fits according to our model are compared to the experimental data in Figs. 8 and 9. Optical tilt angle measurements were fitted according to Eq. (47) with values of $\langle\Theta_r\rangle$ given in Fig. 6 and $\Omega=\Omega_{\text{opt}}$ as a fit parameter. The x-ray tilt angle measurements are fitted by Eq. (48) with values of $\Theta_{r,\text{rms}}$ also given in Fig. 6 and $\Omega=\Omega_{\text{x ray}}$ as a fit parameter (dotted lines). In the case of a two-parameter fit (solid lines) with $\lambda=f(T)$, the reduced temperature τ has to be replaced by the apparent reduced temperature τ_{app}, calculated by Eq. (39) with α_V as an additional fit parameter. The fit parameters (Ω,α_V) obtained from the two-parameter fits are listed in Table I.

In all cases our statistical model gives an excellent description of optical and x-ray tilt angles over the whole Sm-C temperature range with a maximum of only two fit parameters. A two-parameter fit with a significant temperature dependence of λ is necessary in order to achieve a sufficient description of optical measurements in the case of TBBA (Fig. 8) and HSHA (Fig. 9). In contrast to this behavior, the x-ray measurements are also nicely described by one-parameter fits over the whole temperature range. The assumption of a temperature dependence $\lambda=f(T)$ (two-parameter fit, solid lines) leads only to a slight improvement (see Figs. 8 and 9). This behavior is reflected by the temperature coefficients α_V listed in Table I, which are considerably higher for optical tilt angles. To explain this behavior, we may assume in a first approximation that the optical tilt angles are governed by the mean orientation of the highly polarizable mesogenic cores. Obviously, packing density and short range interactions of the mesogenic cores increase with decreasing temperature, leading to a strong temperature dependence of the interaction coefficient λ in the case of optical tilt angles.

The optical tilt angles observed are generally higher than the x-ray tilt angles. Again this behavior can be explained by the strong temperature dependence of the interaction coefficient λ: With decreasing temperature the interaction between the mesogens increases ($\alpha_V>0$) and leads to a stronger tilt of the mesogenic cores with respect to the whole molecule. This behavior is consistent with early qualitative considerations and explains why the optical (mesogen) tilt angles are generally higher than the x-ray (molecule) tilt angles. The differences are extreme in the case of HSHA (Fig. 9), where the hydroxy group laterally attached to the benzylideneaniline mesogen might lead to a very strong attraction between the mesogenic cores.

Comparing the shape of the optical and the x-ray tilt vs temperature curves (Figs. 8 and 9), the square root relation between the x-ray values and the optical values given in Eq. (49) becomes evident: At small tilt angles close to the Sm-A–Sm-C transition, the x-ray values exhibit a steeper increase than the optical values. This situation changes at high tilt angles far below the phase transition.

The fitting routine has been allowed to refine the phase transition temperature T_C, which enters into the reduced temperature τ within a small interval of ± 1 K around the experimental values reported in the literature. The refined values are also listed in Table I and do not deviate significantly from the experimental ones. The small difference in the phase transition temperature of HSHA found for the optical and the x-ray tilt angle measurements (Table I) is probably due to experimental errors involved by different adjustments of the temperature control in the respective experimental setups.

IV. DISCUSSION

Within the framework of the proposed molecular-statistical model, the description of the Sm-A–Sm-C second order phase transition is based on the interaction of molecular tilt vectors $\vec{s}$. An important simplification of the model has been achieved by restricting the treatment on only two, antiparallel directions of $\vec{s}$. The mean value of the molecular tilt vectors serves as a two-component order parameter of the transition. The molecular tilt vectors may physically be interpreted as steric dipoles which are aligned by their own mean-field interactions. The statistical treatment leads to a very simple self-consistent-field equation of state for the Sm-C phase. It has to be stressed that this approach is equivalent to the classical treatment of ferromagnetic phase transitions by Weiss. Consequently, the approach leads to an equation of state which is mathematically analogous to ferromagnetic transitions, however with spin number $S\rightarrow\infty$ [29]. The condition $S\rightarrow\infty$ for a magnetic system without space quantization of the spin moment corresponds to the continuous character of the tilt vector, which may have any length from zero to a maximum length Ω.

The model also corresponds to the early statistical description of nematic liquid crystals given by Born [6]. The basic lack of Born's model was that he applied the polar ordering resulting from the Weiss approach to the nematic director, which is a pseudovector without polarity. In our approach, the nematic director is replaced by the tilt vector of the Sm-C phase, which indeed is a polar vector that undergoes a polar ordering described by the Weiss approach.

Experimental tilt angle data are excellently described by our model over the whole Sm-C temperature range. The essential fit parameter is given by the maximum tilt angle Ω of a preferred molecular axis. In the case of optical tilt angle data, the preferred molecular axis is the principal axis of the polarizability tensor, which is predominantly influenced by

the highly polarizable mesogenic core. In the case of x-ray data, the preferred molecular axis is considered to be the long molecular axis given by the principal axis of molecular inertia. The differences between optical and x-ray data may be comprehensively characterized by the following points.

(i) The different sizes of the optical and the x-ray tilt at a certain temperature are related to different interaction coefficients for the mesogens on one side and the complete molecules on the other. With decreasing temperature, the interaction coefficient of the mesogens exhibits a stronger increase than the ones for the complete molecule. This leads to a higher tilt of the mesogenic cores resulting in a higher value of the optical tilt.

(ii) The different shapes of optical and x-ray tilt angle vs temperature curves result from statistics, because optical and x-ray measurements probe different moments or averages of the tilt angle distribution function.

(iii) The difference between the maximum tilt angles $\Omega_{\mathrm{x\,ray}}$ and Ω_{opt} and their influence on the relation between x-ray and optical tilt is comparatively small.

If the molecular tilt vectors are interpreted as sterical dipoles, the Sm-A–Sm-C transition is a second order phase transition, driven by steric interactions. In this case, the molecular principal axis of inertia probed by x-ray experiments should play a more fundamental role than the dielectric tensor axis. The interaction coefficients λ related to the principal axis of inertia are found to be essentially constant without a significant temperature dependence.

Usually, the Sm-A–Sm-C transition has been described in the framework of a phenomenological Landau theory. In comparison to the Landau approach, we believe that the proposed molecular-statstical model opens an advanced approach to the Sm-A–Sm-C transition for several reasons.

(a) The approach follows the classical mean-field treatment of second order ferromagnetic phase transitions and categorizes the Sm-A–Sm-C transition by basic physical concepts of phase transitions.

(b) The model gives a convenient description of experimental data over the whole Sm-C temperature range involving a smaller number of fit parameters than a Landau-type description of comparable quality.

(c) The fit parameters ($\Omega_{\mathrm{x\,ray}}$, Ω_{opt}, α_V) are open for a physical interpretation in terms of molecular properties and molecular interactions. Roughly speaking, the borderline angle Ω should be related to the molecular geometry and packing while the temperature coefficient α_V corrects oversimplifications of the mean-field approach (e.g., short range interactions). These questions might lead to an advanced understanding of the structure-property relation in Sm-C materials. (A similar interpretation of Landau coefficients seems to be quite a bit more complicated.)

A further analysis of the molecular-statistical model with respect to the thermodynamic functions, critical exponents, and a quantitative comparison to the Landau approach are in progress. Some modification should also allow a description of the ferroelectric Sm-A^*–Sm-C^* transition.

[1] P. H. Hermans and P. Platzek, Kolloid Z. **88**, 68 (1939).
[2] V. Tsvetkov, Acta Physicochim. (USSR) **16**, 132 (1942).
[3] K. K. Kobayashi, J. Phys. Soc. Jpn. **29**, 101 (1970).
[4] K. K. Kobayashi, Mol. Cryst. Liq. Cryst. **13**, 137 (1971).
[5] W. L. McMillan, Phys. Rev. A **4**, 1238 (1971).
[6] M. Born, Ber. Akad. Wiss. Berlin, 614 (1916); Ann. Phys. **55**, 221 (1918).
[7] W. Maier and A. Saupe, Z. Naturforsch. **14a**, 882 (1959); **15a**, 287 (1960).
[8] P. G. de Gennes, Phys. Lett. **A30**, 454 (1969); Mol. Cryst. Liq. Cryst. **12**, 193 (1971).
[9] P. G. de Gennes, Solid State Commun. **10**, 753 (1972).
[10] P. G. de Gennes, Mol. Cryst. Liq. Cryst. **21**, 49 (1973).
[11] R. B. Meyer and T. G. Lubensky, Phys. Rev. A **14**, 2307 (1976).
[12] T. R. Taylor, S. L. Arora, and J. L. Fergason, Phys. Rev. Lett. **25**, 722 (1970).
[13] W. L. McMillan, Phys. Rev. A **8**, 1921 (1973).
[14] W. H. De Jeu, J. Phys. (Paris) **38**, 1265 (1977).
[15] A. Wulf, Phys. Rev. A **11**, 365 (1975).
[16] B. W. Van der Meer and G. Vertogen, J. Phys. (Paris) **40**, 222 (1979).
[17] B. Žekš, Mol. Cryst. Liq. Cryst. **114**, 259 (1984).
[18] C. C. Huang and J. M. Viner, Phys. Rev. A **25**, 3385 (1982).
[19] F. Gießelmann and P. Zugenmaier, Phys. Rev. E **52**, 1762 (1995).
[20] A. I. Derzhanski and A. G. Petrov, Mol. Cryst. Liq. Cryst. **89**, 339 (1982).
[21] N. A. Clark and S. T. Lagerwall, in *Ferroelectric Liquid Crystals*, edited by J. W. Goodby *et al.*, Ferroelectricity and Related Phenomena Vol. 7 (Gordon and Breach, Philadelphia, 1991), p. 6.
[22] P. Weiss, J. Phys. (Paris) **6**, 667 (1907).
[23] W. Gerlach, Z. Elektrochem. **45**, 151 (1939).
[24] S. Chandrasekhar and N. V. Madhusudana, Acta. Crystallogr. **A27**, 303 (1971).
[25] R. L. Humphries, P. G. James, and G. R. Luckhurst, J. Chem. Soc. Faraday Trans. II **68**, 1031 (1972).
[26] S. Kumar, Phys. Rev. A **23**, 3207 (1981).
[27] B. I. Ostrovskii, Sov. Sci. Rev. Sect. A **12**, Pt. 2, 85 (1989).
[28] L. M. Blinov and V. G. Chigrinov, *Electrooptic Effects in Liquid Crystal Materials* (Springer, New York, 1994), p. 7.
[29] H. E. Stanley, *Introduction to Phase Transitions and Critical Phenomena* (Clarendon, Oxford, 1971), p. 82.